

pubs.acs.org/JPCL Letter

Nuclear Quantum Effect and Its Temperature Dependence in Liquid Water from Random Phase Approximation via Artificial Neural Network

Yi Yao* and Yosuke Kanai



Cite This: J. Phys. Chem. Lett. 2021, 12, 6354–6362



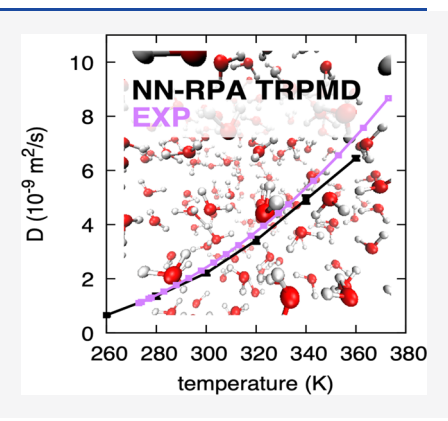
ACCESS

III Metrics & More

Article Recommendations

s Supporting Information

ABSTRACT: We report structural and dynamical properties of liquid water described by the random phase approximation (RPA) correlation together with the exact exchange energy (EXX) within density functional theory. By utilizing thermostated ring polymer molecular dynamics, we examine the nuclear quantum effects and their temperature dependence. We circumvent the computational limitation of performing direct first-principles molecular dynamics simulation at this high level of electronic structure theory by adapting an artificial neural network model. We show that the EXX+RPA level of theory accurately describes liquid water in terms of both dynamical and structural properties.

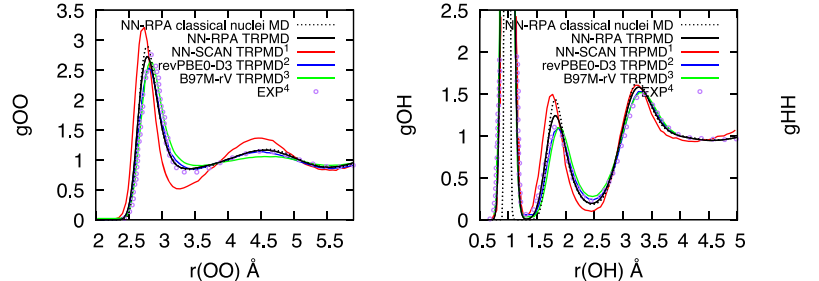


iquid water is arguably the most important condensed dynamical and structural properties under various conditions and settings will have the most overarching impacts in a wide range of fields from atmospheric science to photocatalysis to biochemistry (see, e.g. ref 1 for a recent review). First-principles molecular dynamics (FPMD)^{2,3} simulation provides an exciting prospect for such a grand feat since it does not rely on empirical parameters that need to be tuned for different systems and conditions. Liquid water has been one of the most widely studied systems, and it is arguably the most important application using the FPMD method. 4-36 Yet, an accurate description of liquid water has remained elusive for FPMD simulation. Unlike for classical molecular dynamics simulations in which empirical parameters can be tuned to ensure that the experimental values are obtained for physical properties, 37-39 a number of liquid water properties from FPMD simulation can deviate quite substantially from their corresponding experimental values.21 In recent years, understanding the delicate interplay between the underlying electronic structure theory approximation of FPMD and the classical-particle approximation to nuclei, particularly concerning for protons, has become an important focus in the literature. 40,41 This problem is made further complicated by the plaguing difficulty of achieving statistical convergence for calculated properties in practice because of the significant computational cost of FPMD simulation. 30,34

Density functional theory (DFT) remains the most widely employed electronic structure theory method that is used to drive FPMD simulation because of its appealing balance between the accuracy and efficiency. For FPMD simulation of liquid water based on DFT, most semilocal approximations like the generalize gradient approximation (GGA) to the exchangecorrelation (XC) functional appears inadequate for accurate modeling of liquid water as exhaustively documented in the past decade.²¹ More recent works show that significant improvement can be obtained with the recent nonempirical meta-GGA approximation, SCAN, by Perdew and co-workers, 30,42-45 but not adequate enough for the accuracies often needed for many applications (e.g., the calculated diffusion constant underestimates the experimental value by an order of magnitude³⁰). While the SCAN approximation already includes the intermediate-range van der Waals interaction, a separate correction is needed for the dispersion interaction in general. 44,46 At the same time, some empirically parametrized meta-GGA XC functionals such as B97M-rV^{47,48} approximation appear to perform quite well. B97M-rV meta-GGA approximation is empirically parametrized against extensive data sets together with rVV10 approximation 49,50 for nonlocal correlation. The recent work by Head-Gordon and co-workers showed that B97M-rV meta-GGA approximation can yield great accuracy for various structural and dynamical properties of

Received: May 17, 2021 Accepted: July 1, 2021





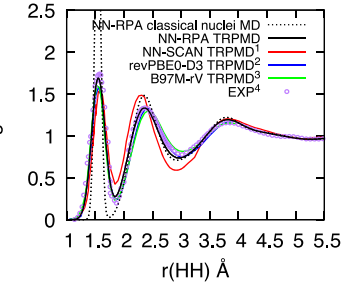


Figure 1. Oxygen—oxygen (left), oxygen—hydrogen (middle), and hydrogen—hydrogen (right) radial distribution function (RDFs) at 300 K from the NN-RPA simulation, in comparison to the experiment and select FPMD references. Referenced data are taken from 1. ref 30, 2. ref 31, 3. ref 33, and 4. ref 86. The statistical error bars in these simulations are smaller than the line width.

liquid water.³³ As for hybrid XC approximations, some great successes have been reported using revPBE0-D3 approximation, in which D3 Grimme's dispersion correction is added to revPBE0 approximation. ^{51–53} In order to illustrate the particular philosophy of achieving increasingly higher accuracy by satisfying more physical constraints (through an increasing number of ingredients from the electronic structure such as electron density, its gradient, kinetic energy density, etc.), Perdew introduced a "Jacob's ladder" analogy for the XC approximation such that climbing the rungs in the ladder would generally lead to a higher accuracy.⁵⁴ Nonempirical variants of the meta-GGA and hybrid XC approximations, which belong to the third and fourth rungs of the Jacob's ladder, by Perdew and co-workers such as SCAN⁴² and PBE0⁵³ approximations do not perform as well as B97M-rV and revPBE0-D3 approximations for liquid water. In the Jacob's ladder, the fifth rung constitutes the XC approximations that depend on the unoccupied/virtual Kohn-Sham states, in addition to those ingredients from the lower rungs (hybrid, meta-GGA, GGA, and LDA). The random phase approximation (RPA) is probably the most wellrecognized approximation that belongs to this fifth rung, and it derives the correlation energy expression through the adiabatic-connection fluctuation-dissipation theorem in the context of DFT. 55-57 The correlation energy is given by the dynamical response function of the noninteracting Kohn-Sham system, and it is generally used together with the exact (Fock) exchange energy from the Kohn-Sham orbitals. Starting with the first practical implementation of the RPA in quantum chemistry by Furche, 58,59 the RPA has become available in various different DFT implementations nowadays. 56,60-65 In particular, the RPA is able to capture the dispersion interaction, 56 and inadequate description of the dispersion interaction is one of crucial shortcomings in many XC approximations for modeling liquid water, often requiring a separate correction for nonlocal correlation. In the context of simulating liquid water, the RPA was used by Del Ben et al. in their NpT Monte Carlo simulation, and the oxygen-oxygen radial distribution function was reported.³⁶ However, without nuclear quantum effects taken into account, it is difficult to assess its agreement with experiments. Quantum-mechanical description of atomic nuclei is indeed a crucial aspect in modeling liquid water using FPMD simulation in addition to the underlying electronic structure theory. 40,41 Starting with the early work by Morrone and Car,³² a number of path-integral approaches have been used in conjunction with FPMD simulation for examining nuclear quantum effects (NQEs) in liquid water. NQEs appear to be quite vital for accurate calculation of structural and dynamical properties of liquid

water. Although it had been long believed that NQEs lead to a less structured liquid water in the context of classical molecular dynamics, 66-68 the seminal work by Harbershon et al. has shown that the less structured liquid water is likely an artifact of using a simple harmonic potential for O-H stretch in popular force field models.⁶⁹ As shown by Markland and co-workers³¹ and also in our recent work, 30 NQEs can lead to a more structured liquid water in FPMD simulations based on hybrid and meta-GGA XC approximations. Furthermore, depending on particular XC approximations employed, NQEs can either accelerate or decelerate the water diffusivity; the diffusion coefficient is decreased with NQEs for revPBE0-D3 hybrid XC approximation³¹ while NQEs slightly increased the diffusion coefficient when B97M-rV meta-GGA XC approximation was used.³³ These recent findings showed that NOEs in liquid water are quite sensitive to the underlying electronic structure theory.³³ Without NQEs properly taken into account, a fortuitous cancellation of errors between an inaccurate potential energy surface and the classical nuclei approximation could be mistaken as accurate electronic structure theory description of liquid water. 31,35 These findings in the past few years therefore call for further studies with higher levels of theory such as the RPA. At the same time, understanding impacts of NQEs together with an advanced electronic structure theory is made further complicated by statistical convergence issues in practice. As pointed out by Gygi and co-workers,³⁴ relatively short FPMD trajectories could lead to unreliable determination of calculated properties from the statistically unconverged ensemble, especially for dynamical properties like diffusion coefficients. In order to overcome the computational difficulty of obtaining FPMD simulation trajectories of hundreds of pico-seconds needed, some have advocated using multiple time-step integration schemes ^{36,70–76} as well as the use of modern machine-learning techniques. ^{30,77–82} In this work, we employ the neural network model 78,83 by Behler and Parrinello to machine-learn the FPMD simulation based on the RPA correlation with the exact exchange (EXX). The Thermostated Ring Polymer Molecular Dynamics (TRPMD) method^{84,85} is used to examine NQEs and its temperature dependence. We show that the EXX+RPA level of theory is able to accurately model liquid water in terms of both dynamical and structural properties. Details of the methodologies are discussed in Computational Method section.

For FPMD simulation, B97M-rV meta-GGA and revPBE0-D3 hybrid XC approximations have shown to yield an accurate oxygen—oxygen radial distribution functions (gOO RDF) at room temperature when NQEs are taken into account via the TRPMD method. Figure 1 shows that our EXX+RPA artificial neural network model ("NN-RPA") also produces an accurate

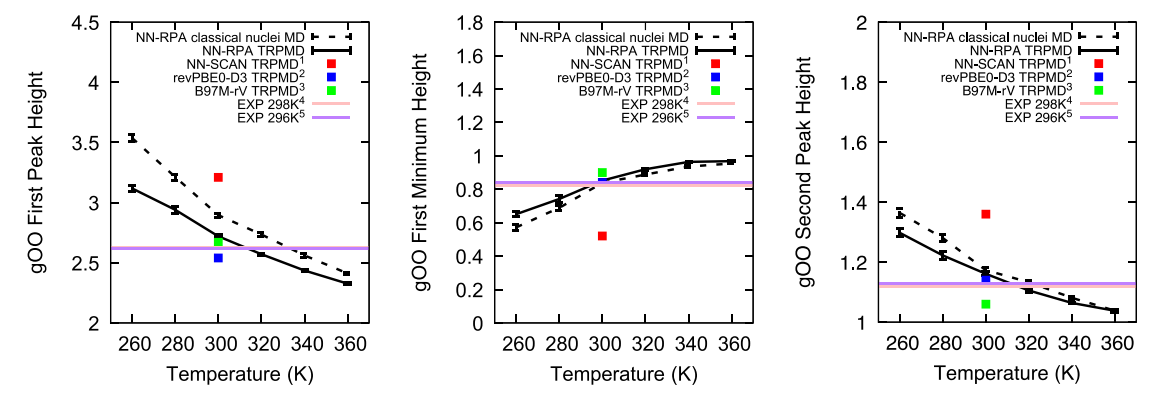


Figure 2. Heights of the first peak (left), the first minimum (middle), and the second peak (right) in the gOO RDF as a function of temperature in the NN-RPA simulation. Experimental references as well as select FPMD references are shown for comparison. Referenced data are taken from 1. ref 30, 2. ref 31, 3. ref 33, 4. ref 87, and 5. ref 86.

gOO RDF at 300 K, and significant improvement over our previous NN-SCAN simulation³⁰ was obtained. Accurate oxygen-hydrogen and hydrogen-hydrogen RDFs (gOH and gHH) are also obtained as can be seen in Figure 1. As expected from the first-principles Monte Carlo simulation with the RPA,36 the classical nuclei approximation with the NN-RPA model results in an overstructured RDFs. Among various gOO RDF features influenced by the NQEs, the first peak is particularly sensitive to the NQEs. Without the NQEs taken into account via the TRPMD, the first peak is noticeably higher than the experimental reference value, indicating an overstructured water. At the same time, the rest of the gOO RDF features are in good agreement with the experimental RDF even without the NQEs. The RDF extrema positions are also in an excellent agreement with the experimental reference. Similar improvement are also evident for the gOH and gHH RDFs when the NQEs are taken into account as seen in Figure 1. For the gOH and gHH RDFs, not only the first peak heights but also the peak widths show great agreement with experiment with the NQEs.

Temperature dependence of the gOO RDF was also examined. Figure 2 shows the temperature dependence of the gOO RDF values for the first peak, the first minimum, and the second peak. The temperature dependence is monotonic over the simulation temperature range of 260~360 K, and the first RDF peak shows the most significant temperature dependence. The NQE on the first peak remains quite significant at all temperatures while the NQEs on the first minimum and the second peak are relatively small. An artificial elevation of the simulation temperature is often used as a computationally efficient protocol for mimicking some aspects of NQEs in modeling liquid water using classical nuclei MD simulation as discussed in ref 30. Figure 2 indicates that the artificial elevation of ~30K in classical nuclei MD simulation would yield the experimental gOO RDF for the first peak, which is an important marker for water molecules' local structural environment.

Accurate calculation of the self-diffusion coefficient in FPMD simulation remains a significant challenge. Marsalek and Markland reported a highly accurate diffusion coefficient using revPBE0-D3 hybrid XC level of theory in 2017.³¹ Interestingly, their FPMD simulation at room temperature showed that the diffusion coefficient decreased by ~15% when NQEs were taken into account via the TRPMD approach. Habershon and coworkers have previously explained such somewhat counterintuitive observation in terms of the delicate balance between

intermolecular and intramolecular nuclear quantum effects. ⁶⁹ At the same time, Ruiz Pestana et al. found that NQEs lead to a slightly faster diffusivity when B97M-rV meta-GGA was employed, and the same TRPMD approach was used for taking into account NQEs in 2018.33 Our recent SCAN meta-GGA work³⁰ showed that, for the temperatures lower than 300 K, NQEs lead to a \sim 10% reduction in the diffusion coefficient. For the temperatures higher than 300 K, NQEs slow down the diffusivity by 15%~20%. These observations show that the NQE on the diffusivity is exceptionally sensitive to the underlying electronic structure theory. Unlike for revPBE0-D3 hybrid XC approximation, the SCAN meta-GGA work, ³⁰ however, did not produce a reasonable diffusion coefficient even with NQEs.³⁰ Figure 3 shows the temperature dependence of the self-diffusion coefficient from the NN-RPA simulation, and NQEs are incorporated via the TRPMD method. The reported values in Figure 3 include the finite size error correction⁸⁸ based on temperature-dependent experimental viscosity of liquid water⁸⁹ as done in the same way in refs 30,31,33 The diffusion

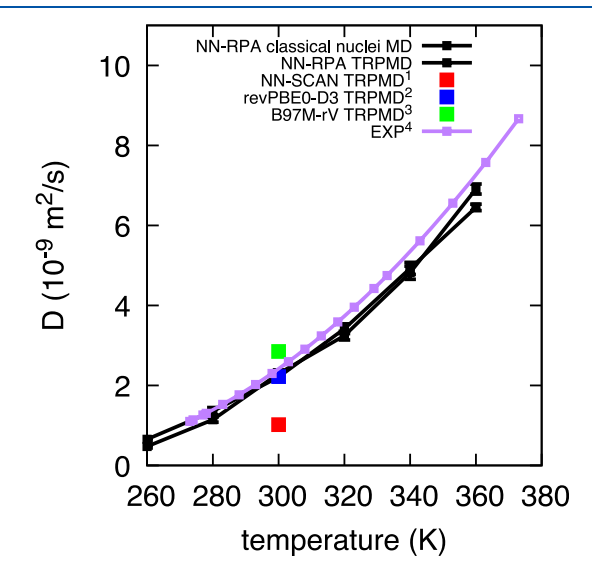


Figure 3. Temperature dependence of the diffusion coefficient from the NN-RPA simulation, in comparison to the experimental values reported in ref 90 The finite size error correction⁸⁸ based on temperature-dependent experimental viscosity of liquid water⁸⁹ is included. Select FPMD references are also shown for comparison. Referenced data are taken from 1. ref 30, 2. ref 31, 3. ref 33, and 4. ref 90.

coefficients are found to be in an excellent agreement with the experimental temperature-dependent diffusion coefficient, 90 and the NQE on the diffusion coefficient is found to be negligibly small, being on the same order of magnitude as the statistical errors. The temperature dependence is found to be much more significant on the diffusion coefficient. This observation again underscores the notion that the NQE on the diffusion coefficient is very sensitive to the underlying electronic structure theory as reported in the recent FPMD works. 30,31,33

Unlike for many molecular dynamics simulations with commonly used force fields, NQEs have been found to slow down the rotational dynamics at room temperature in FPMD simulation at the revPBE0-D3 hybrid XC level of theory. ³¹ Our recent SCAN meta-GGA work showed a nontrivial temperature dependence for the NQE on the rotational dynamics, ³⁰ and agreement of the rotational relaxation constants to the corresponding experimental values was quite unsatisfactory. Table 1 shows the relaxation time constants calculated from the

Table 1. Relaxation Time Constants for the Second-Order Orientational Correlation of Individual Water Molecules Using the H–H Vector $(\tau^{\rm HH})$, O–H Vector $(\tau^{\rm OH})$, and the Dipole Vector $(\tau^{\prime\prime})$ from the Classical Nuclei MD and TRPMD at 300 K, in Comparison to the NN-SCAN Results, revPBE0-D3 Results, and the Experimental Values at Room Temperature

	$ au^{ m HH}$	$ au^{ m OH}$	$ au^{\mu}$
NN-RPA classical nucl.	2.6 (0.2)	2.2 (0.1)	1.7 (0.1)
NN-RPA TRPMD	2.8 (0.2)	2.3 (0.1)	1.8 (0.1)
NN-SCAN classical nucl.a	21.5 (3.1)	15.7 (2.2)	12.9 (1.9)
NN-SCAN TRPMD ^a	18.1 (3.9)	16.0 (4.3)	12.0 (3.6)
revPBE0-D3 classical nucl. b	2.01	1.73	1.35
revPBE0-D3 TRPMD ^b	2.62	2.13	1.67
$experiment^c$	1.6-2.5	1.95	1.90
^a Ref 30. ^b Ref 31. ^c Refs 91–94.			

NN-RPA simulation for the second-order orientational correlation function for the H-H vector, the O-H vector, and the dipole vector of individual water molecules at 300 K, in comparison to the revPBE0-D3 result³¹ and to the experimental values. SCAN meta-GGA results, the

EXX+RPA level of theory yields a considerable improvement, and great agreement with experimental values is obtained. At the same time, we find that the NQE decelerates the rotational dynamics rather negligibly, being on the same order of magnitude as the statistical errors. Figure 4 shows the temperature dependence of the relaxation time constants; notably, having quantum nuclei plays a rather minor role for the rotational dynamics, while the temperature dependence is much more significant.

Unlike the direct FPMD simulations using the maximally localized Wannier functions, 95 the use of the artificial neural network does not allow us to obtain IR spectra in our NN-RPA simulation. Instead of computing the IR spectra, the vibrational density of states (VDOS) was calculated from the Fourier transform of the velocity-velocity autocorrelation function as shown in Figure 5. In agreement with the earlier FPMD simulations using the revPBE0-D3 hybrid and B97M-rV meta-GGA XC approximations, 31,33 the most prominent change due to NQEs is on the O-H stretching mode region, and the NQEs red-shift the O-H stretch peak to 3553 cm⁻¹ from 3795 cm⁻¹ in the NN-RPA simulation. As widely appreciated in the literature, the broadening of the O-H stretching peak is likely due to an artifact of the TRPMD method. 31,33,96 The NQEs also affect the O-H bending mode region (experimentally ~ 1637 cm⁻¹ in the IR measurement) and the libration mode region, but only slightly. Temperature dependence of the NQEs on both O-H stretching and bending modes is rather minor (see Figure 5). The libration mode exhibits a negligibly small NQE for the vibrational power spectrum, and this observation appears at odds with a noticeable blue-shift observed in the IR spectra for the revPBE0-D3 hybrid XC and B97M-rV meta-GGA simulations. 31,33

In pursuit of an accurate description of liquid water via first-principles molecular dynamics (FPMD) simulation, the description at the random phase approximation (RPA) level of theory was examined within density functional theory (DFT) formalism. The RPA correlation energy together with the exact exchange energy (EXX) based on the Kohn–Sham orbitals was employed, belonging to the fifth rung of the so-called Jacob's ladder of DFT by Perdew. S4 Artificial neural network model representation was adapted to circumvent the computational limitation of performing direct FPMD simulation at this advanced level of electronic structure theory, and the

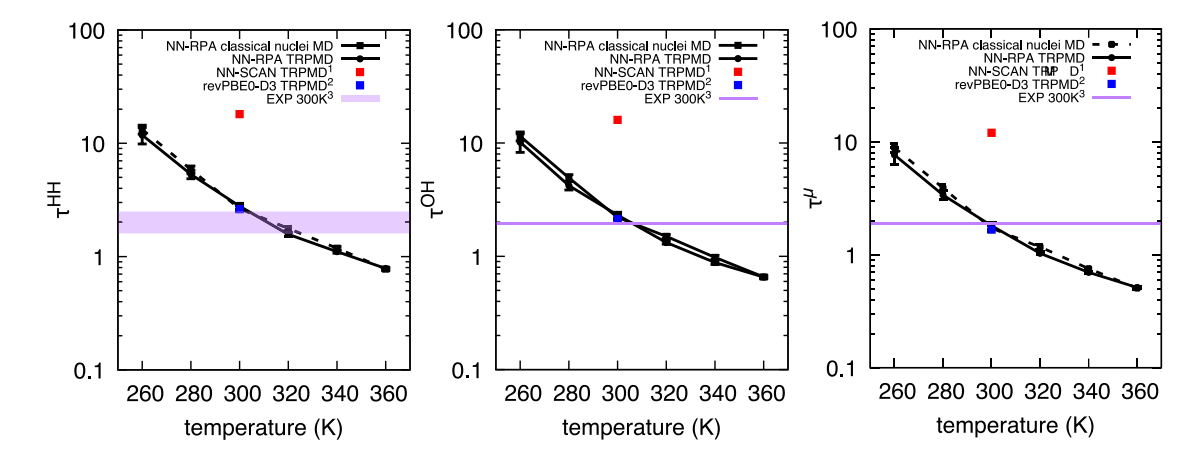
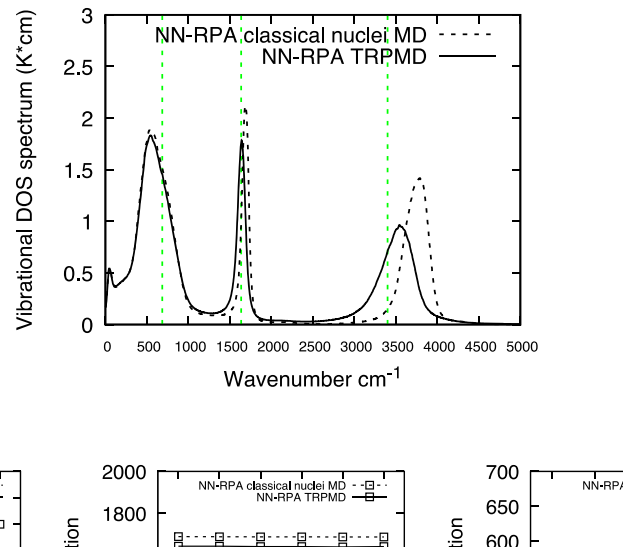
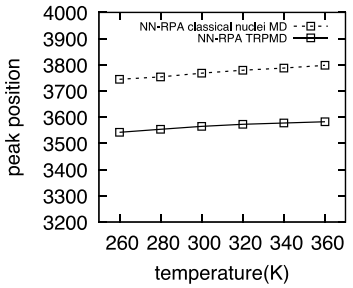
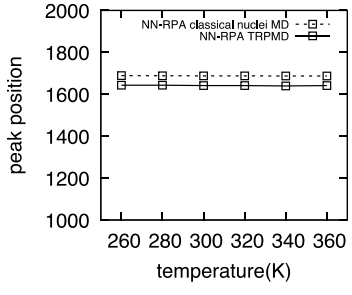


Figure 4. Temperature dependence of the relaxation time constants for the second-order orientational correlation of individual water molecules using H–H vector (left), O–H vector (middle), and dipole vector (right) from the classical nuclei MD and TRPMD. The experimental values at 300 K are also shown for comparison. Note the log scale in the *y*-axis. Referenced data are taken from 1. ref 30, 2. ref 31, and 3. refs 91–94.







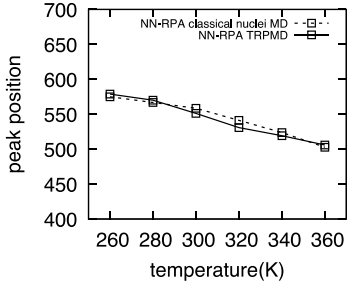


Figure 5. (Top) The vibrational density of states (VDOS) of liquid water at 300 K from the NN-RPA simulation. The green dashed vertical lines indicate the peaks in the experimental IR spectrum. ⁹⁷ (Bottom) The temperature dependence of the vibrational peak positions is shown for the O–H stretch mode (left), H–O–H bending mode (middle), and the libration mode (right).

thermostated ring polymer molecular dynamics (TRPMD) method was used for taking into account nuclear quantum effects (NQEs). This EXX+RPA level of the theory was found to yield an accurate description of liquid water overall. The simulation shows great quantitative agreement with experimental values for the radial distribution functions, the diffusion coefficients, and the rotational relaxation times. The NQEs noticeably lower the first peak height of the oxygen-oxygen RDF, yielding an excellent agreement with the experimental data for this important structural indicator. For the self-diffusion coefficient and the rotational relaxation constants of water molecules, the NQEs appear to play a rather minor role across the temperature range of 260~360 K. The NQEs also result in a significant redshift of the O-H stretch peak by as much as 200 cm⁻¹ in the vibrational spectrum. NQEs play a surprisingly small effect on liquid water dynamics at this advanced level of theory, except for the intramolecular vibrational dynamics. Given the appreciable NQEs on these dynamical properties observed previously for the revPBE0-D3 hybrid XC³¹ as well as for B97MrV³³ and SCAN meta-GGA³⁰ XC approximations (despite their differing effects), the present finding may seem rather surprising at first. At the same time, recent works show that NQEs depend quite sensitively on the underlying electronic structure theory approximation to the extent that the water dynamics can be either accelerated or decelerated, depending on the potential energy surface. Our present work again underscores that the NQEs in liquid water, especially for dynamical properties like the diffusion coefficient, are quite sensitive to the underlying electronic structure theory. ^{30,31,33}

In spite of the exciting results obtained in this work, given the long and sometimes controversial history of this topic, we must

remain cautious about a possible cancellation of errors between the underlying potential energy from the electronic structure theory and quantum nuclear description via TRPMD method as well as the use of artificial neural network. In addition to improving XC approximation within DFT formalism, other electronic structure theories are increasingly employed in FPMD in recent years even though these simulations are still limited in terms of NQEs and simulation size/length. The second-order Møller-Plesset perturbation theory (MP2), for instance, has been employed in FPMD simulation of liquid water with different types of approximations (e.g., Fragment-based MP2, SCS-MP2) by a few different groups. 17,98–100 Still, one important drawback of MP2 calculation, especially for simulation of liquid water, is that it does not correctly capture the dispersion interaction, ¹⁰¹ and a separate correction scheme might be necessary. ^{102–104} Others have also employed an approximated coupled-cluster theory method within the QM/ MM scheme, 105 and variational quantum Monte Carlo method has been used for the FPMD simulation as well.²⁰ In the near future, "gold standard" methods such as CCSD(T) and diffusion quantum Monte Carlo might become feasible for modeling liquid water, providing a computational means for validating the EXX+RPA description of liquid water, which yields great agreement for experimentally measured properties.

COMPUTATIONAL METHOD

The random phase approximation (RPA) correlation energy and the exact (Fock) exchange (EXX) energy were calculated from the Kohn–Sham eigenfunctions based on the PBE GGA XC approximation⁵¹ within density functional theory (DFT). We use the CP2K code to perform the EXX+RPA calculation¹⁰⁵

within the mixed Gaussian and Planewaves (GPW) formalism. $^{62,63,106-108}$ The TZVP Gaussian basis set was used 109,110 together with the planewave cutoff of 800 Ry for the electron density, and the Goedecker-Teter-Hutter (GTH) pseudopotential was used. 111 The resolution of identity approach was used for reducing the computational cost of evaluating the four center integrals.⁶³ Since it is presently not feasible to perform RPAbased FPMD simulation with the planewave basis set, SCAN meta-GGA XC was used for assessing the convergence of the TZVP basis set. The TZVP basis set result was compared with the converged planewave basis set result. 112 The convergence test is discussed in Supporting Information. The artificial neural network (NN) force field was developed following our earlier work for SCAN meta-GGA XC approximation³⁰ in the exact same manner as discussed in Supporting Information. We used the Atomic Energy NETwork code 113 to train the NN force field, and an excellent agreement was obtained for the oxygenoxygen radial distribution function available from the firstprinciples Monte Carlo simulation³⁶ as shown in Supporting Information. The i-PI code¹¹⁴ was interfaced with the Atomic Energy NETwork code to perform classical nuclei MD and TRPMD simulations. In all cases, we used a cubic simulation cell of 11.8172 Å with the periodic boundary conditions with 55 water molecules, corresponding to the experimental water density of 0.997 g/cm² at 300 K. For the classical nuclei MD simulations, we used the integration step size of 0.5 fs with the Nose-Hoover thermostat. 115-117 For the TRPMD simulations, we used the integration step size of 0.25 fs, and the path integral Langevin equation global (PILE-G) thermostat 118 was used for the temperature control. The TRPMD simulations employ 32 beads for sampling the path integral as shown sufficient previously.41 For the calculation of diffusion coefficient, this standard approach combining the TRPMD and the PILE-G thermostat has been used in recent works on NQEs in liquid water, 31,33,112 and it has been validated to yield a precise diffusion coefficient.84

ASSOCIATED CONTENT

Supporting Information

The Supporting Information is available free of charge at https://pubs.acs.org/doi/10.1021/acs.jpclett.1c01566.

Parameters and training sets for the neural network model as well as other computational details (PDF)

NN-RPA potential (ZIP)

Training data (ZIP)

AUTHOR INFORMATION

Corresponding Author

Yi Yao — Department of Chemistry, University of North Carolina at Chapel Hill, Durham, North Carolina 27599, United States; Department of Mechanical Engineering and Materials Science, Duke University, Durham, North Carolina 27708, United States; oorcid.org/0000-0002-9957-6979; Email: yy244@duke.edu

Author

Yosuke Kanai — Department of Chemistry, University of North Carolina at Chapel Hill, Durham, North Carolina 27599, United States; ocid.org/0000-0002-2320-4394

Complete contact information is available at: https://pubs.acs.org/10.1021/acs.jpclett.1c01566

Notes

The authors declare no competing financial interest.

ACKNOWLEDGMENTS

The work is partly supported by the National Science Foundation under Grant No. CHE-1954894 and OAC-1740204. An award of computer time was provided by the Innovative and Novel Computational Impact on Theory and Experiment (INCITE) program. This research used resources of the Argonne Leadership Computing Facility, which is a U.S. DOE Office of Science User Facility supported under Contract No. DE-AC02-06CH11357.

REFERENCES

- (1) Brini, E.; Fennell, C. J.; Fernandez-Serra, M.; Hribar-Lee, B.; Lukšič, M.; Dill, K. A. How Water's Properties Are Encoded in Its Molecular Structure and Energies. *Chem. Rev.* **2017**, *117* (19), 12385–12414.
- (2) Car, R.; Parrinello, M. Unified Approach for Molecular Dynamics and Density-Functional Theory. *Phys. Rev. Lett.* **1985**, *55* (22), 2471–2474
- (3) Hafner, J. A joint effort with lasting impact. *Nat. Mater.* **2010**, 9 (9), 690–692.
- (4) Laasonen, K.; Sprik, M.; Parrinello, M.; Car, R. Ab initio"liquid water. J. Chem. Phys. 1993, 99 (11), 9080–9089.
- (5) Sprik, M.; Hutter, J.; Parrinello, M. Ab initio molecular dynamics simulation of liquid water: Comparison of three gradient-corrected density functionals. *J. Chem. Phys.* **1996**, *105* (3), 1142–1152.
- (6) Silvestrelli, P. L.; Parrinello, M. Structural, electronic, and bonding properties of liquid water from first principles. *J. Chem. Phys.* **1999**, *111* (8), 3572–3580.
- (7) Chen, B.; Ivanov, I.; Klein, M. L.; Parrinello, M. Hydrogen bonding in water. *Phys. Rev. Lett.* **2003**, *91* (21), 215503.
- (8) Grossman, J. C.; Schwegler, E.; Draeger, E. W.; Gygi, F.; Galli, G. Towards an assessment of the accuracy of density functional theory for first principles simulations of water. *J. Chem. Phys.* **2004**, *120* (1), 300–311.
- (9) Kuo, I-F. W.; Mundy, C. J.; McGrath, M. J.; Siepmann, J. I.; VandeVondele, J.; Sprik, M.; Hutter, J.; Chen, B.; Klein, M. L.; Mohamed, F.; Krack, M.; Parrinello, M. Liquid water from first principles: Investigation of different sampling approaches. *J. Phys. Chem. B* **2004**, *108* (34), 12990–12998.
- (10) Schwegler, E.; Grossman, J. C.; Gygi, F.; Galli, G. Towards an assessment of the accuracy of density functional theory for first principles simulations of water. II. *J. Chem. Phys.* **2004**, *121* (11), 5400–5409.
- (11) Fernández-Serra, M.; Ferlat, G.; Artacho, E. Two exchange-correlation functionals compared for first-principles liquid water. *Mol. Simul.* **2005**, *31* (5), 361–366.
- (12) Lee, H.-S.; Tuckerman, M. E. Structure of liquid water at ambient temperature from ab initio molecular dynamics performed in the complete basis set limit. *J. Chem. Phys.* **2006**, *125* (15), 154507.
- (13) Lee, H.-S.; Tuckerman, M. E. Dynamical properties of liquid water from ab initio molecular dynamics performed in the complete basis set limit. *J. Chem. Phys.* **2007**, *126* (16), 164501.
- (14) Lu, D.; Gygi, F.; Galli, G. Dielectric properties of ice and liquid water from first-principles calculations. *Phys. Rev. Lett.* **2008**, *100* (14), 147601.
- (15) Zhang, C.; Donadio, D.; Gygi, F.; Galli, G. First principles simulations of the infrared spectrum of liquid water using hybrid density functionals. *J. Chem. Theory Comput.* **2011**, *7* (5), 1443–1449.
- (16) Lin, I.-C.; Seitsonen, A. P.; Tavernelli, I.; Rothlisberger, U. Structure and Dynamics of Liquid Water from ab Initio Molecular Dynamics Comparison of BLYP, PBE, and revPBE Density Functionals with and without van der Waals Corrections. *J. Chem. Theory Comput.* **2012**, *8* (10), 3902–3910.

- (17) Del Ben, M.; Schönherr, M.; Hutter, J. r.; VandeVondele, J. Bulk liquid water at ambient temperature and pressure from MP2 theory. *J. Phys. Chem. Lett.* **2013**, 4 (21), 3753–3759.
- (18) Bankura, A.; Karmakar, A.; Carnevale, V.; Chandra, A.; Klein, M. L. Structure, dynamics, and spectral diffusion of water from first-principles molecular dynamics. *J. Phys. Chem. C* **2014**, *118* (50), 29401–29411.
- (19) Morales, M. A.; Gergely, J. R.; McMinis, J.; McMahon, J. M.; Kim, J.; Ceperley, D. M. Quantum Monte Carlo benchmark of exchange-correlation functionals for bulk water. *J. Chem. Theory Comput.* **2014**, *10* (6), 2355–2362.
- (20) Zen, A.; Luo, Y.; Mazzola, G.; Guidoni, L.; Sorella, S. Ab initio molecular dynamics simulation of liquid water by quantum Monte Carlo. *J. Chem. Phys.* **2015**, *142* (14), 144111.
- (21) Gillan, M. J.; Alfè, D.; Michaelides, A. Perspective: How good is DFT for water? J. Chem. Phys. 2016, 144 (13), 130901.
- (22) Morawietz, T.; Singraber, A.; Dellago, C.; Behler, J. How van der Waals interactions determine the unique properties of water. *Proc. Natl. Acad. Sci. U. S. A.* **2016**, *113* (30), 8368–8373.
- (23) Ambrosio, F.; Miceli, G.; Pasquarello, A. Structural, Dynamical, and Electronic Properties of Liquid Water: A Hybrid Functional Study. *J. Phys. Chem. B* **2016**, *120* (30), 7456–7470.
- (24) Chen, M.; Ko, H.-Y.; Remsing, R. C.; Calegari Andrade, M. F.; Santra, B.; Sun, Z.; Selloni, A.; Car, R.; Klein, M. L.; Perdew, J. P.; Wu, X. Ab initio theory and modeling of water. *Proc. Natl. Acad. Sci. U. S. A.* **2017**, *114* (41), 10846–10851.
- (25) Machida, M.; Kato, K.; Shiga, M. Nuclear quantum effects of light and heavy water studied by all-electron first principles path integral simulations. *J. Chem. Phys.* **2018**, *148* (10), 102324.
- (26) Morawietz, T.; Marsalek, O.; Pattenaude, S. R.; Streacker, L. M.; Ben-Amotz, D.; Markland, T. E. The interplay of structure and dynamics in the Raman spectrum of liquid water over the full frequency and temperature range. *J. Phys. Chem. Lett.* **2018**, *9* (4), 851–857.
- (27) Sun, Z.; Zheng, L.; Chen, M.; Klein, M. L.; Paesani, F.; Wu, X. Electron-hole theory of the effect of quantum nuclei on the X-ray absorption spectra of liquid water. *Phys. Rev. Lett.* **2018**, *121* (13), 137401.
- (28) Zheng, L.; Chen, M.; Sun, Z.; Ko, H.-Y.; Santra, B.; Dhuvad, P.; Wu, X. Structural, electronic, and dynamical properties of liquid water by ab initio molecular dynamics based on SCAN functional within the canonical ensemble. *J. Chem. Phys.* **2018**, *148* (16), 164505.
- (29) Gaiduk, A. P.; Gustafson, J.; Gygi, F.; Galli, G. First-Principles Simulations of Liquid Water Using a Dielectric-Dependent Hybrid Functional. *J. Phys. Chem. Lett.* **2018**, 9 (11), 3068–3073.
- (30) Yao, Y.; Kanai, Y. Temperature dependence of nuclear quantum effects on liquid water via artificial neural network model based on SCAN meta-GGA functional. *J. Chem. Phys.* **2020**, *153* (4), No. 044114.
- (31) Marsalek, O.; Markland, T. E. Quantum dynamics and spectroscopy of ab initio liquid water: The interplay of nuclear and electronic quantum effects. *J. Phys. Chem. Lett.* **2017**, 8 (7), 1545–1551.
- (32) Morrone, J. A.; Car, R. Nuclear quantum effects in water. *Phys. Rev. Lett.* **2008**, *101* (1), No. 017801.
- (33) Ruiz Pestana, L.; Marsalek, O.; Markland, T. E.; Head-Gordon, T. The quest for accurate liquid water properties from first principles. *J. Phys. Chem. Lett.* **2018**, 9 (17), 5009–5016.
- (34) Dawson, W.; Gygi, F. Equilibration and analysis of first-principles molecular dynamics simulations of water. *J. Chem. Phys.* **2018**, *148* (12), 124501.
- (35) Ruiz Pestana, L.; Mardirossian, N.; Head-Gordon, M.; Head-Gordon, T. Ab initio molecular dynamics simulations of liquid water using high quality meta-GGA functionals. *Chemical Science* **2017**, 8 (5), 3554–3565.
- (36) Del Ben, M.; Hutter, J.; VandeVondele, J. Probing the structural and dynamical properties of liquid water with models including non-local electron correlation. *J. Chem. Phys.* **2015**, *143* (5), No. 054506.
- (37) Wang, L.-P.; Head-Gordon, T.; Ponder, J. W.; Ren, P.; Chodera, J. D.; Eastman, P. K.; Martinez, T. J.; Pande, V. S. Systematic improvement of a classical molecular model of water. *J. Phys. Chem. B* **2013**, *117* (34), 9956–9972.

- (38) Wang, L.-P.; Martinez, T. J.; Pande, V. S. Building force fields: An automatic, systematic, and reproducible approach. *J. Phys. Chem. Lett.* **2014**, *5* (11), 1885–1891.
- (39) Qiu, Y.; Nerenberg, P. S.; Head-Gordon, T.; Wang, L.-P. Systematic optimization of water models using liquid/vapor surface tension data. *J. Phys. Chem. B* **2019**, *123* (32), 7061–7073.
- (40) Markland, T. E.; Ceriotti, M. Nuclear quantum effects enter the mainstream. *Nature Reviews Chemistry* **2018**, 2 (3), 0109.
- (41) Ceriotti, M.; Fang, W.; Kusalik, P. G.; McKenzie, R. H.; Michaelides, A.; Morales, M. A.; Markland, T. E. Nuclear quantum effects in water and aqueous systems: Experiment, theory, and current challenges. *Chem. Rev.* **2016**, *116* (13), 7529–7550.
- (42) Sun, J.; Ruzsinszky, A.; Perdew, J. P. Strongly constrained and appropriately normed semilocal density functional. *Phys. Rev. Lett.* **2015**, *115* (3), No. 036402.
- (43) Chen, M.; Ko, H.-Y.; Remsing, R. C.; Calegari Andrade, M. F.; Santra, B.; Sun, Z.; Selloni, A.; Car, R.; Klein, M. L.; Perdew, J. P.; Wu, X. Ab initio theory and modeling of water. *Proc. Natl. Acad. Sci. U. S. A.* **2017**, *114* (41), 10846–10851.
- (44) Wiktor, J.; Ambrosio, F.; Pasquarello, A. Note: Assessment of the SCAN+rVV10 functional for the structure of liquid water. *J. Chem. Phys.* **2017**, *147* (21), 216101.
- (45) LaCount, M. D.; Gygi, F. Ensemble first-principles molecular dynamics simulations of water using the SCAN meta-GGA density functional. *J. Chem. Phys.* **2019**, *151* (16), 164101.
- (46) Peng, H.; Yang, Z.-H.; Perdew, J. P.; Sun, J. Versatile van der Waals Density Functional Based on a Meta-Generalized Gradient Approximation. *Phys. Rev. X* **2016**, *6* (4), No. 041005.
- (47) Mardirossian, N.; Ruiz Pestana, L.; Womack, J. C.; Skylaris, C.-K.; Head-Gordon, T.; Head-Gordon, M. Use of the rVV10 nonlocal correlation functional in the B97M-V density functional: Defining B97M-rV and related functionals. *J. Phys. Chem. Lett.* **2017**, 8 (1), 35–40.
- (48) Mardirossian, N.; Head-Gordon, M. Mapping the genome of meta-generalized gradient approximation density functionals: The search for B97M-V. *J. Chem. Phys.* **2015**, *142* (7), No. 074111.
- (49) Sabatini, R.; Gorni, T.; De Gironcoli, S. Nonlocal van der Waals density functional made simple and efficient. *Phys. Rev. B: Condens. Matter Mater. Phys.* **2013**, 87 (4), No. 041108.
- (50) Vydrov, O. A.; Van Voorhis, T. Nonlocal van der Waals density functional: The simpler the better. *J. Chem. Phys.* **2010**, *133* (24), 244103.
- (51) Perdew, J. P.; Burke, K.; Ernzerhof, M. Generalized gradient approximation made simple. *Phys. Rev. Lett.* **1996**, 77 (18), 3865.
- (52) Zhang, Y.; Yang, W. Comment on Generalized Gradient Approximation Made Simple. *Phys. Rev. Lett.* **1998**, *80* (4), 890–890.
- (53) Perdew, J. P.; Ernzerhof, M.; Burke, K. Rationale for mixing exact exchange with density functional approximations. *J. Chem. Phys.* **1996**, 105 (22), 9982–9985.
- (54) Perdew, J. P.; Schmidt, K. Jacob's ladder of density functional approximations for the exchange-correlation energy. *AIP Conference Proceedings* **2001**, *577*, 1–20.
- (55) Langreth, D. C.; Perdew, J. P. Exchange-correlation energy of a metallic surface: Wave-vector analysis. *Phys. Rev. B* 1977, 15 (6), 2884.
- (56) Ren, X.; Rinke, P.; Joas, C.; Scheffler, M. Random-phase approximation and its applications in computational chemistry and materials science. *J. Mater. Sci.* **2012**, *47* (21), 7447–7471.
- (57) Fuchs, M.; Gonze, X. Accurate density functionals: Approaches using the adiabatic-connection fluctuation-dissipation theorem. *Phys. Rev. B: Condens. Matter Mater. Phys.* **2002**, *65* (23), 235109.
- (58) Furche, F. Molecular tests of the random phase approximation to the exchange-correlation energy functional. *Phys. Rev. B: Condens. Matter Mater. Phys.* **2001**, 64 (19), 195120.
- (59) Furche, F. Developing the random phase approximation into a practical post-Kohn—Sham correlation model. *J. Chem. Phys.* **2008**, *129* (11), 114105.
- (60) Kaltak, M.; Klimes, J.; Kresse, G. Low scaling algorithms for the random phase approximation: Imaginary time and Laplace transformations. *J. Chem. Theory Comput.* **2014**, *10* (6), 2498–2507.

- (61) Kaltak, M.; Klimeš, J.; Kresse, G. Cubic scaling algorithm for the random phase approximation: Self-interstitials and vacancies in Si. *Phys. Rev. B: Condens. Matter Mater. Phys.* **2014**, 90 (5), No. 054115.
- (62) Del Ben, M.; Hutter, J. r.; VandeVondele, J. Electron correlation in the condensed phase from a resolution of identity approach based on the Gaussian and plane waves scheme. *J. Chem. Theory Comput.* **2013**, 9 (6), 2654–2671.
- (63) Del Ben, M.; Schütt, O.; Wentz, T.; Messmer, P.; Hutter, J.; VandeVondele, J. Enabling simulation at the fifth rung of DFT: Large scale RPA calculations with excellent time to solution. *Comput. Phys. Commun.* **2015**, *187*, 120–129.
- (64) Nguyen, H.-V.; de Gironcoli, S. Efficient calculation of exact exchange and RPA correlation energies in the adiabatic-connection fluctuation-dissipation theory. *Phys. Rev. B: Condens. Matter Mater. Phys.* **2009**, 79 (20), 205114.
- (65) Miyake, T.; Aryasetiawan, F.; Kotani, T.; van Schilfgaarde, M.; Usuda, M.; Terakura, K. Total energy of solids: An exchange and random-phase approximation correlation study. *Phys. Rev. B: Condens. Matter Mater. Phys.* **2002**, *66* (24), 245103.
- (66) Hernández de la Peña, L.; Kusalik, P. Quantum effects in light and heavy liquid water: A rigid-body centroid molecular dynamics study. *J. Chem. Phys.* **2004**, *121* (12), 5992–6002.
- (67) Miller, T. F., III; Manolopoulos, D. E. Quantum diffusion in liquid water from ring polymer molecular dynamics. *J. Chem. Phys.* **2005**, *123* (15), 154504.
- (68) Hernández de la Peña, L.; Kusalik, P. G. Quantum effects in liquid water and ice: Model dependence. *J. Chem. Phys.* **2006**, *125* (5), No. 054512.
- (69) Habershon, S.; Markland, T. E.; Manolopoulos, D. E. Competing quantum effects in the dynamics of a flexible water model. *J. Chem. Phys.* **2009**, *131* (2), No. 024501.
- (70) Anglada, E.; Junquera, J.; Soler, J. M. Efficient mixed-force first-principles molecular dynamics. *Phys. Rev. E: Stat. Phys., Plasmas, Fluids, Relat. Interdiscip. Top.* **2003**, *68* (5), No. 055701.
- (71) Geng, H. Y. Accelerating ab initio path integral molecular dynamics with multilevel sampling of potential surface. *J. Comput. Phys.* **2015**, 283, 299–311.
- (72) Marsalek, O.; Markland, T. E. Ab initio molecular dynamics with nuclear quantum effects at classical cost: Ring polymer contraction for density functional theory. *J. Chem. Phys.* **2016**, *144* (5), No. 054112.
- (73) Tuckerman, M.; Berne, B. J.; Martyna, G. J. Reversible multiple time scale molecular dynamics. *J. Chem. Phys.* **1992**, *97* (3), 1990–2001.
- (74) Kapil, V.; VandeVondele, J.; Ceriotti, M. Accurate molecular dynamics and nuclear quantum effects at low cost by multiple steps in real and imaginary time: Using density functional theory to accelerate wavefunction methods. *J. Chem. Phys.* **2016**, *144* (5), No. 054111.
- (75) Guidon, M.; Schiffmann, F.; Hutter, J.; VandeVondele, J. Ab initio molecular dynamics using hybrid density functionals. *J. Chem. Phys.* **2008**, *128* (21), 214104.
- (76) Luehr, N.; Markland, T. E.; Martínez, T. J. Multiple time step integrators in ab initio molecular dynamics. *J. Chem. Phys.* **2014**, *140* (8), No. 084116.
- (77) Behler, J. Perspective: Machine learning potentials for atomistic simulations. *J. Chem. Phys.* **2016**, *145* (17), 170901.
- (78) Behler, J.; Parrinello, M. Generalized Neural-Network Representation of High-Dimensional Potential-Energy Surfaces. *Phys. Rev. Lett.* **2007**, 98 (14), 146401.
- (79) Zhang, L.; Han, J.; Wang, H.; Car, R.; E, W. Deep Potential Molecular Dynamics: A Scalable Model with the Accuracy of Quantum Mechanics. *Phys. Rev. Lett.* **2018**, *120* (14), 143001.
- (80) Imbalzano, G.; Anelli, A.; Giofré, D.; Klees, S.; Behler, J.; Ceriotti, M. Automatic selection of atomic fingerprints and reference configurations for machine-learning potentials. *J. Chem. Phys.* **2018**, 148 (24), 241730.
- (81) Cheng, B.; Engel, E. A.; Behler, J.; Dellago, C.; Ceriotti, M. Ab initio thermodynamics of liquid and solid water. *Proc. Natl. Acad. Sci. U. S. A.* **2019**, *116* (4), 1110–1115.

- (82) Behler, J. First Principles Neural Network Potentials for Reactive Simulations of Large Molecular and Condensed Systems. *Angew. Chem., Int. Ed.* **2017**, *56* (42), 12828–12840.
- (83) Behler, J. Atom-centered symmetry functions for constructing high-dimensional neural network potentials. *J. Chem. Phys.* **2011**, *134* (7), No. 074106.
- (84) Rossi, M.; Ceriotti, M.; Manolopoulos, D. E. How to remove the spurious resonances from ring polymer molecular dynamics. *J. Chem. Phys.* **2014**, *140* (23), 234116.
- (85) Rossi, M.; Liu, H.; Paesani, F.; Bowman, J.; Ceriotti, M. Communication: On the consistency of approximate quantum dynamics simulation methods for vibrational spectra in the condensed phase. *The Journal of Chemical Physics* **2014**, *141*, 181101.
- (86) Soper, A.; Benmore, C. Quantum differences between heavy and light water. *Phys. Rev. Lett.* **2008**, *101* (6), No. 065502.
- (87) Brookes, D. H.; Head-Gordon, T. Family of oxygen—oxygen radial distribution functions for water. *J. Phys. Chem. Lett.* **2015**, *6* (15), 2938–2943.
- (88) Yeh, I.-C.; Hummer, G. System-size dependence of diffusion coefficients and viscosities from molecular dynamics simulations with periodic boundary conditions. *J. Phys. Chem. B* **2004**, *108* (40), 15873–15879.
- (89) Zaytsev, I. D.; Aseyev, G. G. Properties of aqueous solutions of electrolytes; CRC press: 1992.
- (90) Tofts, P.; Lloyd, D.; Clark, C.; Barker, G.; Parker, G.; McConville, P.; Baldock, C.; Pope, J. Test liquids for quantitative MRI measurements of self-diffusion coefficient in vivo. *Magn. Reson. Med.* **2000**, 43 (3), 368–374.
- (91) Winkler, K.; Lindner, J.; Bürsing, H.; Vöhringer, P. Ultrafast Raman-induced Kerr-effect of water: Single molecule versus collective motions. *J. Chem. Phys.* **2000**, *113* (11), 4674–4682.
- (92) Lawrence, C.; Skinner, J. Vibrational spectroscopy of HOD in liquid D 2 O. III. Spectral diffusion, and hydrogen-bonding and rotational dynamics. *J. Chem. Phys.* **2003**, *118* (1), 264–272.
- (93) Rezus, Y.; Bakker, H. On the orientational relaxation of HDO in liquid water. *J. Chem. Phys.* **2005**, *123* (11), 114502.
- (94) Tan, H.-S.; Piletic, I. R.; Fayer, M. Orientational dynamics of water confined on a nanometer length scale in reverse micelles. *J. Chem. Phys.* **2005**, *122* (17), 174501.
- (95) Marzari, N.; Vanderbilt, D. Maximally localized generalized Wannier functions for composite energy bands. *Phys. Rev. B: Condens. Matter Mater. Phys.* **1997**, *56* (20), 12847–12865.
- (96) Rossi, M.; Liu, H.; Paesani, F.; Bowman, J.; Ceriotti, M. Communication: On the consistency of approximate quantum dynamics simulation methods for vibrational spectra in the condensed phase. *J. Chem. Phys.* **2014**, *141* (18), 181101.
- (97) Chase, M. W., Jr; Tables, N.-J. T. Data reported in NIST standard reference database 69, June 2005 release: NIST Chemistry WebBook. *J. Phys. Chem. Ref. Data, Monograph* **1998**, *9*, 1–1951.
- (98) Liu, J.; He, X.; Zhang, J. Z. Structure of liquid water—a dynamical mixture of tetrahedral and 'ring-and-chain'like structures. *Phys. Chem. Chem. Phys.* **2017**, *19* (19), 11931–11936.
- (99) Willow, S. Y.; Salim, M. A.; Kim, K. S.; Hirata, S. Ab initio molecular dynamics of liquid water using embedded-fragment second-order many-body perturbation theory towards its accurate property prediction. *Sci. Rep.* **2015**, *5* (1), 14358.
- (100) Willow, S. Y.; Zeng, X. C.; Xantheas, S. S.; Kim, K. S.; Hirata, S. Why is MP2-water "cooler" and "denser" than DFT-water? *J. Phys. Chem. Lett.* **2016**, *7* (4), 680–684.
- (101) Sinnokrot, M. O.; Sherrill, C. D. Highly accurate coupled cluster potential energy curves for the benzene dimer: sandwich, T-shaped, and parallel-displaced configurations. *J. Phys. Chem. A* **2004**, *108* (46), 10200–10207.
- (102) Heßelmann, A. Improved supermolecular second order Møller—Plesset intermolecular interaction energies using time-dependent density functional response theory. *J. Chem. Phys.* **2008**, *128* (14), 144112.

- (103) Pitonak, M.; Heßelmann, A. Accurate intermolecular interaction energies from a combination of MP2 and TDDFT response theory. *J. Chem. Theory Comput.* **2010**, *6* (1), 168–178.
- (104) Rezac, J.; Greenwell, C.; Beran, G. J. Accurate Noncovalent Interactions via Dispersion-Corrected Second-Order Møller–Plesset Perturbation Theory. *J. Chem. Theory Comput.* **2018**, *14* (9), 4711–4721.
- (105) Eshuis, H.; Yarkony, J.; Furche, F. Fast computation of molecular random phase approximation correlation energies using resolution of the identity and imaginary frequency integration. *J. Chem. Phys.* **2010**, 132 (23), 234114.
- (106) VandeVondele, J.; Krack, M.; Mohamed, F.; Parrinello, M.; Chassaing, T.; Hutter, J. Quickstep: Fast and accurate density functional calculations using a mixed Gaussian and plane waves approach. *Comput. Phys. Commun.* **2005**, *167* (2), 103–128.
- (107) Hutter, J.; Iannuzzi, M.; Schiffmann, F.; VandeVondele, J. cp2k: atomistic simulations of condensed matter systems. Wiley Interdisciplinary Reviews: Computational Molecular Science 2014, 4 (1), 15–25.
- (108) Kühne, T. D.; Iannuzzi, M.; Del Ben, M.; Rybkin, V. V.; Seewald, P.; Stein, F.; Laino, T.; Khaliullin, R. Z.; Schütt, O.; Schiffmann, F.; Golze, D.; Wilhelm, J.; Chulkov, S.; Bani-Hashemian, M. H.; Weber, V.; Borštnik, U.; Taillefumier, M.; Jakobovits, A. S.; Lazzaro, A.; Pabst, H.; Müller, T.; Schade, R.; Guidon, M.; Andermatt, S.; Holmberg, N.; Schenter, G. K.; Hehn, A.; Bussy, A.; Belleflamme, F.; Tabacchi, G.; Glöß, A.; Lass, M.; Bethune, I.; Mundy, C. J.; Plessl, C.; Watkins, M.; VandeVondele, J.; Krack, M.; Hutter, J. CP2K: An electronic structure and molecular dynamics software package Quickstep: Efficient and accurate electronic structure calculations. *J. Chem. Phys.* 2020, 152 (19), 194103.
- (109) Dunning, T. H., Jr Gaussian basis sets for use in correlated molecular calculations. I. The atoms boron through neon and hydrogen. J. Chem. Phys. 1989, 90 (2), 1007–1023.
- (110) Del Ben, M.; Hutter, J. r.; VandeVondele, J. Second-order Møller–Plesset perturbation theory in the condensed phase: An efficient and massively parallel Gaussian and plane waves approach. *J. Chem. Theory Comput.* **2012**, 8 (11), 4177–4188.
- (111) Goedecker, S.; Teter, M.; Hutter, J. Separable dual-space Gaussian pseudopotentials. *Phys. Rev. B: Condens. Matter Mater. Phys.* **1996**, 54 (3), 1703.
- (112) Yao, Y.; Kanai, Y. Plane-wave pseudopotential implementation and performance of SCAN meta-GGA exchange-correlation functional for extended systems. *J. Chem. Phys.* **2017**, 146 (22), 224105.
- (113) Artrith, N.; Urban, A. An implementation of artificial neural-network potentials for atomistic materials simulations: Performance for TiO2. *Comput. Mater. Sci.* **2016**, *114*, 135–150.
- (114) Ceriotti, M.; More, J.; Manolopoulos, D. E. i-PI: A Python interface for ab initio path integral molecular dynamics simulations. *Comput. Phys. Commun.* **2014**, *185* (3), 1019–1026.
- (115) Nosé, S. A unified formulation of the constant temperature molecular dynamics methods. *J. Chem. Phys.* **1984**, *81* (1), 511–519.
- (116) Nosé, S. A molecular dynamics method for simulations in the canonical ensemble. *Mol. Phys.* **1984**, *52* (2), 255–268.
- (117) Hoover, W. G. Canonical dynamics: Equilibrium phase-space distributions. *Phys. Rev. A: At., Mol., Opt. Phys.* **1985**, 31 (3), 1695.
- (118) Ceriotti, M.; Parrinello, M.; Markland, T. E.; Manolopoulos, D. E. Efficient stochastic thermostatting of path integral molecular dynamics. *J. Chem. Phys.* **2010**, *133* (12), 124104.